


 Cite this: *RSC Adv.*, 2018, **8**, 17677

 Received 10th January 2018
 Accepted 23rd April 2018

DOI: 10.1039/c8ra00280k

rsc.li/rsc-advances

Deactivation by HCl of $\text{CeO}_2\text{--MoO}_3\text{/TiO}_2$ catalyst for selective catalytic reduction of NO with NH_3

 Ye Jiang,  ^{*a} Mingyuan Lu,^a Shaojun Liu,^b Changzhong Bao,^a Guitao Liang,^a Chengzhen Lai,^a Weiyun Shi^a and Shiyuan Ma^a

The effect of HCl on a $\text{CeO}_2\text{--MoO}_3\text{/TiO}_2$ catalyst for the selective catalytic reduction of NO with NH_3 was investigated with BET, XRD, $\text{NH}_3\text{-TPD}$, $\text{H}_2\text{-TPR}$, XPS and catalytic activity measurements. The results showed that HCl had an inhibiting effect on the activity of the $\text{CeO}_2\text{--MoO}_3\text{/TiO}_2$ catalyst. The deactivation by HCl of the $\text{CeO}_2\text{--MoO}_3\text{/TiO}_2$ catalyst could be attributed to pore blockage, weakened interaction among ceria, molybdenum and titania, reduction in surface acidity and degradation of redox ability. The $\text{Ce}^{3+}\text{/Ce}^{4+}$ redox cycle was damaged because unreactive Ce^{3+} in the form of CeCl_3 lost the ability to be converted to active Ce^{4+} in the SCR reaction. In addition, a decrease in the amount of chemisorbed oxygen and the concentrations of surface Ce and Mo was also responsible for the deactivation by HCl of the $\text{CeO}_2\text{--MoO}_3\text{/TiO}_2$ catalyst.

1. Introduction

The selective catalytic reduction (SCR) of NO_x with NH_3 is an efficient technology for the removal of NO_x in flue gas from stationary sources.¹ $\text{V}_2\text{O}_5\text{-WO}_3\text{(MoO}_3\text{)}/\text{TiO}_2$ catalysts have been widely used in the last few decades.^{2,3} In recent years, great attention has been paid to develop environment-friendly vanadium-free catalysts for SCR applications mainly owing to the toxicity of vanadium.^{4,5} Cerium-based catalysts are regarded as promising candidates due to the high oxygen storage capacity and excellent redox properties of CeO_2 .^{4,6,7} Many researchers have developed numerous cerium-based metal oxide catalysts, which possessed good SCR activity, such as $\text{MoO}_3\text{/CeO}_2\text{-ZrO}_2$,⁸ Cu-Ce-Ti oxide,^{6,9} Mn-Ce-Ti oxide,¹⁰ etc. Our group prepared a $\text{CeO}_2\text{-MoO}_3\text{/TiO}_2$ catalyst using a single step sol-gel method, which exhibited high SCR activity and resistance to 10% H_2O and 1000 ppm SO_2 .¹¹ However, from the point of view of industrial applications, further studies are still required to clarify their adaptability to other components in flue gas from stationary sources, such as alkali (earth) metals, heavy metals, HCl, etc.

It is well known that HCl is widely present in the flue gas from coal-fired boilers and municipal solid waste (MSW) incinerators. The effect of HCl on SCR catalyst has been investigated by several researchers. Chen *et al.*¹² attributed the deactivation by HCl of $\text{V}_2\text{O}_5\text{/TiO}_2$ catalyst to the formation of volatile vanadium chlorides and NH_4Cl . Lisi *et al.*¹³ reported

that HCl suppressed the SCR activity of commercial $\text{V}_2\text{O}_5\text{-WO}_3\text{/TiO}_2$ catalyst due to the formation of new acid sites showing a lower activity compared to the original one. Yang *et al.*¹⁴ proposed that Cl could inhibit the adsorption of NH_3 and NO_x species, thereby leading to the deactivation of Ce/TiO_2 . On the contrary, Hou *et al.*¹⁵ found that HCl had a positive effect on the catalytic activity of $\text{V}_2\text{O}_5\text{/AC}$ catalyst at 150 °C. As for the effect of HCl on $\text{CeO}_2\text{-MoO}_3\text{/TiO}_2$ catalyst for the SCR of NO with NH_3 , there were few reports to our knowledge till now.

In this work, the effect of HCl on $\text{CeO}_2\text{-MoO}_3\text{/TiO}_2$ catalyst was investigated for the SCR of NO with NH_3 . A series of characterizations, including BET, XRD, XPS, $\text{NH}_3\text{-TPD}$ and $\text{H}_2\text{-TPR}$, were performed to provide an insight into the substantial change in $\text{CeO}_2\text{-MoO}_3\text{/TiO}_2$ catalyst caused by HCl.

2. Experimental

2.1. Catalyst preparation

The $\text{CeO}_2\text{-MoO}_3\text{/TiO}_2$ catalyst was prepared by a single step sol-gel method as reported in our previous study.¹¹ The mass ratio of $\text{CeO}_2 : \text{MoO}_3 : \text{TiO}_2$ was 20 : 10 : 100. All chemicals used in the catalyst preparation were purchased from Sino-pharm Chemical Reagent Corp. (Shanghai, China). Except that titanium butoxide (TBOT) was chemically pure, the other reagents were of analytical grade. TBOT, anhydrous ethanol, deionized water, 65–68 wt% nitric acid, cerium nitrate hexahydrate ($\text{Ce}(\text{NO}_3)_3 \cdot 6\text{H}_2\text{O}$) and ammonium molybdate tetrahydrate ($(\text{NH}_4)_6\text{Mo}_7\text{O}_24 \cdot 4\text{H}_2\text{O}$) were mixed at a molar ratio of 1 : 35 : 19 : 2 : 0.1 : 0.1. After continuously stirred for 3 h at room temperature, the solution was kept at 80 °C for 24 h to form xerogel. The obtained xerogel were milled and sieved out,

^aCollege of Pipeline and Civil Engineering, China University of Petroleum, 66 Changjiang West Road, Qingdao 266580, P. R. China. E-mail: jiangye@upc.edu.cn; Fax: +86-532-86981882; Tel: +86-532-86981767

^bState Key Laboratory of Clean Energy Utilization, Zhejiang University, 32 Zheda Road, Hangzhou 310027, China



followed by calcination at 500 °C for 5 h in static air. The catalyst was denoted as CMT.

The HCl-loaded $\text{CeO}_2\text{-MoO}_3\text{/TiO}_2$ catalysts were prepared by impregnation *via* incipient wetness with appropriate hydrochloric acid solution on CMT. The mixture was aged for 24 h and dried at 80 °C for 12 h. The HCl-loaded $\text{CeO}_2\text{-MoO}_3\text{/TiO}_2$ catalysts were denoted as CMT x , where x represented the molar ratio of Cl and Ce.

2.2. Catalyst characterization

BET surface area, total pore volume and average pore diameter were measured by N_2 adsorption and desorption at −196 °C with ASAP2020-M (Micromeritics Instrument Corp.). Prior to the measurement, the sample was degassed in vacuum at 300 °C for 4 h.

X-ray diffraction (XRD) measurement was carried out with on a X'Pert PRO diffractometer (Panalytical Corp.) with $\text{Cu K}\alpha$ radiation at 40 kV and 40 mA.

X-ray photoelectron spectroscopy (XPS) data were obtained with a Thermo ESCALAB 250 spectrometer using monochromated $\text{Al K}\alpha$ X-rays ($hm = 1486.6$ eV) as a radiation source at 150 W. Sample charging effects were eliminated by correcting the observed spectra with the C 1s binding energy (BE) value of 284.6 eV.

Temperature programmed desorption of NH_3 ($\text{NH}_3\text{-TPD}$) and temperature programmed reduction of H_2 ($\text{H}_2\text{-TPR}$) were performed on a FINESORB-3010 chemisorption analyzer (FINETEC Instruments Corp.) with 0.1 g of the catalysts with a thermal conductivity detector (TCD). For $\text{NH}_3\text{-TPD}$, the sample was pretreated at 500 °C in He for 1 h. After cooled down, it was exposed in a 0.5% NH_3 /He (30 mL min^{−1}) gas flow for 1 h, followed by flushing with He for 1 h. Finally, the sample was heated up to 700 °C with the rate of 10 °C min^{−1} in He. $\text{H}_2\text{-TPR}$ were carried out in the flow of H_2 (10%) in Ar (30 mL min^{−1})

from room temperature to 800 °C with the heating rate of 10 °C min^{−1}.

2.3. SCR activity test

The activity measurements were carried out in a fixed-bed quartz reactor (i.d. = 8 mm) using 0.23 g catalyst with 60–100 mesh at atmospheric pressure in the temperature range of 150–500 °C. The feed gas contained 1000 ppm NO, 1000 ppm NH_3 , 3 vol% O_2 , 10% H_2O (when used), 500 ppm SO_2 (when used) and N_2 as balance gas. The total flow rate was 500 mL min^{−1}, corresponding to a gas hourly space velocity (GHSV) of 150 000 h^{−1}. The concentrations of NO, SO_2 and O_2 were continuously monitored by a gas analyzer (350 Pro, Testo). The concentrations of NO_2 and N_2O were recorded by a FT-IR gas analyzer (DX-4000, Gasmet). The NO conversion and N_2 selectivity of catalysts were calculated by:¹⁶

$$\text{NO conversion}(\%) = \frac{[\text{NO}]_{\text{in}} - [\text{NO}]_{\text{out}}}{[\text{NO}]_{\text{in}}} \times 100 \quad (1)$$

$$\text{N}_2 \text{ selectivity}(\%) = \left(1 - \frac{[\text{NO}_2]_{\text{out}} + 2[\text{N}_2\text{O}]_{\text{out}}}{[\text{NO}]_{\text{in}} - [\text{NO}]_{\text{out}}} \right) \times 100 \quad (2)$$

3. Results and discussion

3.1. $\text{NH}_3\text{-SCR}$ performance

Fig. 1 shows the $\text{NH}_3\text{-SCR}$ performance of the fresh and HCl-loaded CMT. It could be seen from Fig. 1(a) that the catalytic activity of CMT declined and its active temperature window was shortened with increasing HCl loadings in the temperature range of 150–500 °C. Furthermore, it seemed that the inhibiting effect of HCl on the SCR activity of CMT was more obvious below 300 °C. As for the N_2 selectivity, there was hardly a difference among the three samples at temperatures from

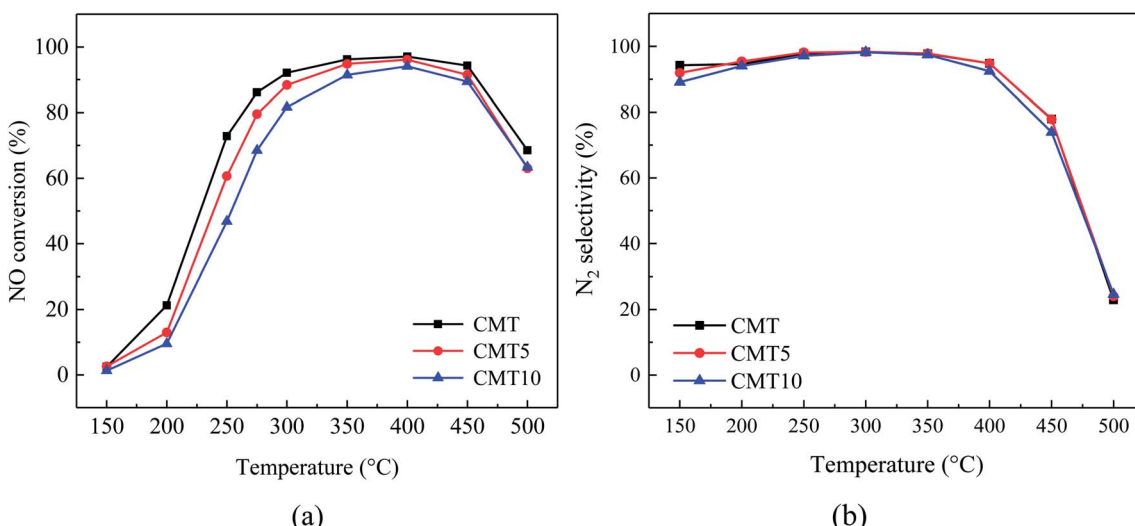


Fig. 1 SCR activity (a) and N_2 selectivity (b) of different samples as a function of reaction temperature. Reaction conditions: $[\text{NO}] = [\text{NH}_3] = 1000$ ppm, $[\text{O}_2] = 3\%$, balance N_2 , GHSV = 150 000 h^{−1}.

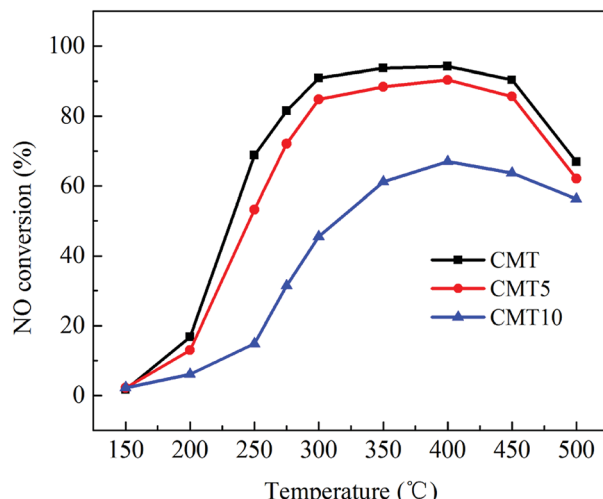


Fig. 2 Effect of H_2O on NO conversion over different samples. Reaction conditions: $[\text{NO}] = [\text{NH}_3] = 1000 \text{ ppm}$, $[\text{O}_2] = 3\%$, $[\text{H}_2\text{O}] = 10\%$, balance N_2 and GHSV = $150\,000 \text{ h}^{-1}$.

250 °C to 350 °C. The N_2 selectivity of CMT10 decreased slightly below 250 °C and at 350–450 °C in comparison with those of CMT and CMT5. It could be seen that HCl loadings had little influence on the N_2 selectivity of CMT.

The effect of H_2O on the SCR activities of the fresh and HCl-loaded CMT was investigated and the results are shown in Fig. 2. Compared with Fig. 1 and 2, it was found that CMT10 suffered much more serious deactivation than the other samples. The presence of H_2O suppressed the NO removal process over SCR catalysts by competing with NH_3 adsorption on the reaction sites or occupying the oxygen vacancies in active species.^{6,17,18} The existence of HCl on the surface of CMT was likely to aggravate the competitive adsorption of H_2O with NH_3 and the positioning of the oxygen vacancies in Ce species.

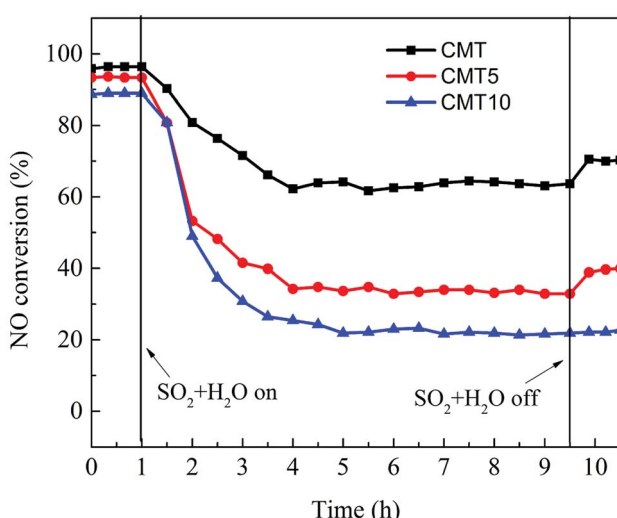


Fig. 3 Effect of H_2O and SO_2 on NO conversion for different catalyst samples as a function of reaction temperature. Reaction conditions: $[\text{NO}] = [\text{NH}_3] = 1000 \text{ ppm}$, $[\text{O}_2] = 3\%$, $[\text{H}_2\text{O}] = 10\%$, $[\text{SO}_2] = 500 \text{ ppm}$, balance N_2 and GHSV = $150\,000 \text{ h}^{-1}$.

Fig. 3 displays the co-effect of H_2O and SO_2 on the SCR of NO with NH_3 over the fresh and HCl-loaded CMT. The presence of SO_2 and H_2O led to a rapid decrease in the SCR activities of the three samples to different extents. After about 4 hours, their activities became stable. It was clear that the resistance of CMT against SO_2 and H_2O declined with increasing the loadings of HCl. The deactivation by SO_2 of Ce-based oxide SCR catalysts was believed to result from the formation of sulfate species on their surface, including NH_4HSO_4 , $\text{Ce}(\text{SO}_4)_2$ and $\text{Ce}_2(\text{SO}_4)_3$.^{17,19,20} In the presence of O_2 , SO_2 and H_2O might react with NH_3 to produce NH_4HSO_4 . NH_4HSO_4 could accumulate on catalyst surface and further cover active sites.¹⁹ On the other hand, SO_2 might combine with Ce species on catalyst surface in the presence of O_2 to form high thermally stable $\text{Ce}(\text{SO}_4)_2$ and $\text{Ce}_2(\text{SO}_4)_3$. They could hinder the $\text{Ce}^{4+}/\text{Ce}^{3+}$ redox cycle and inhibit the formation and adsorption of surface nitrate species.¹⁹ After SO_2 and H_2O were cut off from the feed gas, the NO conversions over CMT and CMT5 increased slightly, while no obvious change was observed in the NO conversion over CMT10. It indicated that there might exist NH_4HSO_4 on the surface of CMT and CMT5. After removing SO_2 and H_2O , unstable NH_4HSO_4 volatilized or decomposed. The deactivation of the three samples was largely caused by $\text{Ce}(\text{SO}_4)_2$ and $\text{Ce}_2(\text{SO}_4)_3$. The presence of HCl might promote the formation of the two sulfate species, thereby resulting in more serious deactivation of CMT10.

3.2. Characterization of catalysts

3.2.1 BET and XRD analysis. According to the BET results, it was found that the BET surface area of different samples decreased by the following order: CMT ($99.06 \text{ m}^2 \text{ g}^{-1}$) > CMT5 ($88.76 \text{ m}^2 \text{ g}^{-1}$) > CMT10 ($81.49 \text{ m}^2 \text{ g}^{-1}$). It was clear that the BET surface area of CMT decreased with increasing Cl loadings, which was consistent with the catalytic activity (as shown in Fig. 1). Fig. 4 shows the pore size distribution of the samples. It could be seen that the pore sizes of CMT increased with increasing Cl loadings while the pore volumes fell gradually. This meant that a portion of small mesopores might be blocked

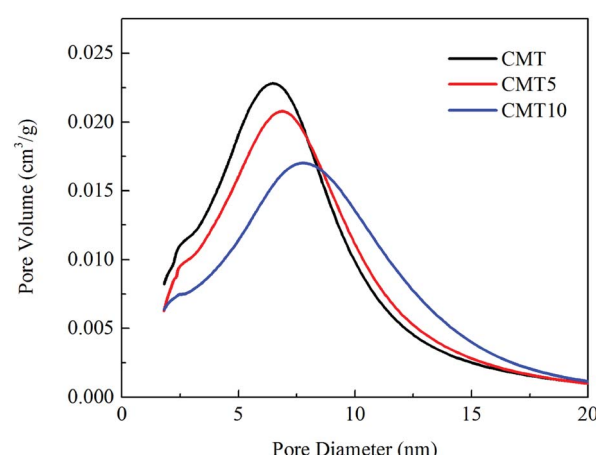


Fig. 4 Pore size distributions of the catalyst samples.

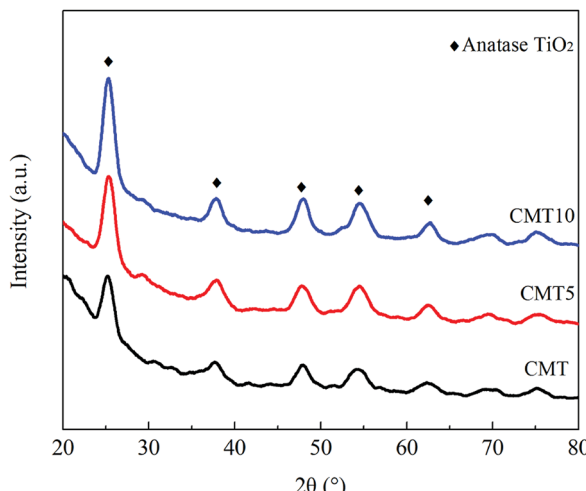


Fig. 5 XRD patterns of the catalyst samples.

by chloride species. Wang *et al.*²¹ found the similar phenomena in the study on the effect of F or Cl on Mn/TiO₂ catalyst.

The XRD patterns of the fresh and HCl-loaded CMT are presented in Fig. 5. Only the diffraction peaks ascribed to anatase TiO₂ were detected, while the characteristic peaks of CeO₂ and MoO₃ were not observed. This demonstrated that the presence of HCl had no obvious impact on the dispersion of CeO₂ and MoO₃ on the surface of TiO₂. CeO₂ and MoO₃ were still highly dispersed and existed as amorphous or highly dispersed species in CMT. However, the intensity of the diffraction peaks due to anatase TiO₂ was found to increase with increasing Cl loadings. This meant that the presence of HCl served to weaken the interaction among CeO₂, MoO₃ and TiO₂, thereby resulting in the deactivation of CMT.

3.2.2 XPS analysis. The surface atomic concentrations of the catalyst samples are summarized in Table 1. The addition of HCl led to the decrease in the amount of reactive Ce and Mo atoms on the catalyst surface, which was in line with the catalytic activity. In addition, it was found that the measured Cl concentration on the catalyst surface was far lower than its nominal one. This might be due to its extraordinary high volatility.²²

As shown in Fig. 6, the binding energies of Ti 2p_{1/2} and Ti 2p_{3/2} in different catalysts were about 464.5 and 458.5 eV, respectively.²³ It suggested that Ti in CMT and CMT10 existed in its highest oxidation state(IV).²⁴ There was no significant change in the peak position among the two samples, but the intensities of both peaks increased after the introduction of Cl, which was

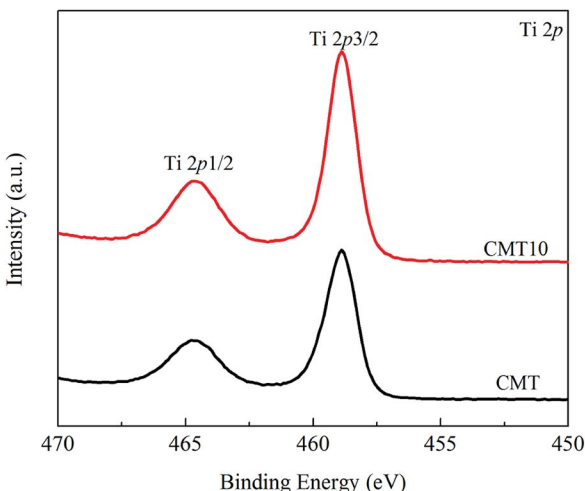


Fig. 6 XPS spectra of Ti 2p for the catalyst samples.

in accordance with the XRD results. This meant that there existed an interaction between HCl and Ti.

After a curve-fitting procedure in Fig. 7, the spectra of O 1s can be deconvoluted into two peaks. The peak at about 529.7–530.1 eV could be assigned to lattice oxygen (denoted as O_α) and the other one at about 531.1–531.4 eV could be related to chemisorbed oxygen (denoted as O_β) from oxide defects or hydroxyl-like groups.^{25,26} After treated by HCl, the O_β/O ratio decreased from 35.21% to 23.62%, which was in good agreement with the catalytic activity. O_β was considered to be more active in SCR reaction than O_α because of its higher mobility.²⁷ As a result, the SCR activity of CMT decreased after loading HCl.

The deconvoluted Ce 3d XPS results of the catalyst samples are shown in Fig. 8. The peaks labeled u, u'', u''' and v, v'', v''' are assigned to Ce⁴⁺, while u' and v' are attributed to Ce³⁺.^{28,29} The atomic ratio of Ce³⁺/Ce, calculated by the area of the corresponding peaks, increased from 31.81% to 34.76%. It indicated that the presence of HCl led to the increase in the amount of Ce³⁺ and the decrease in the amount of Ce⁴⁺ on the catalyst

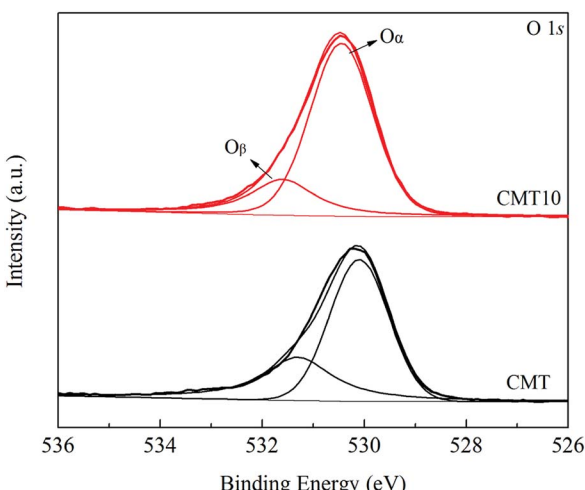


Table 1 Surface element compositions of the catalyst samples determined by XPS

Sample	Surface atomic concentration (%)						
	O	Ti	Mo	Ce	Cl	O _β /O	Ce ³⁺ /Ce
CMT	66.53	27.71	3.09	2.68	—	35.21	31.81
CMT10	64.73	29.42	2.64	2.01	1.20	23.62	34.76

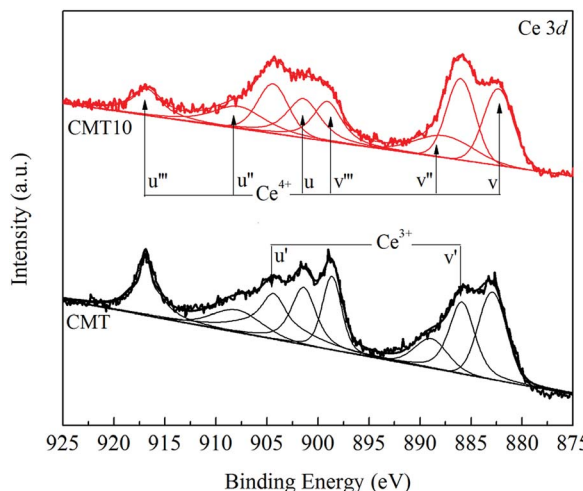


Fig. 8 XPS spectra of Ce 3d for the catalyst samples.

surface. It is widely accepted that Ce^{3+} can create a charge imbalance and form oxygen vacancies and unsaturated chemical bonds, which is helpful for the formation of chemisorbed oxygen on the catalyst surface.³⁰ However, it was unexpected that the increase in the amount of Ce^{3+} due to the presence of HCl did not promote the formation of chemisorbed oxygen. On the contrary, the amount of chemisorbed oxygen decreased. It might be supposed that not all Ce^{3+} species could act as a promoter on SCR activity.

Fig. 9 illustrates the XPS spectra of Cl 2p in CMT10. The peak appearing at 198.4 eV was assigned to Cl^- .³¹ According to the handbook of X-ray photoelectron spectroscopy,³² it could be inferred that CeCl_3 molecules might form on the surface of CMT10. It could be speculated that a fraction of CeO_2 might react with HCl according to the following reaction:

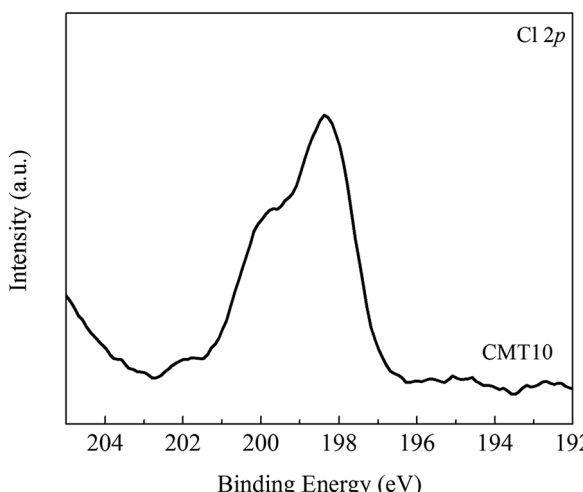
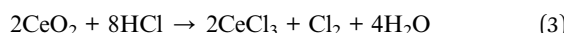


Fig. 9 XPS spectra of Cl 2p for the CMT10 sample.

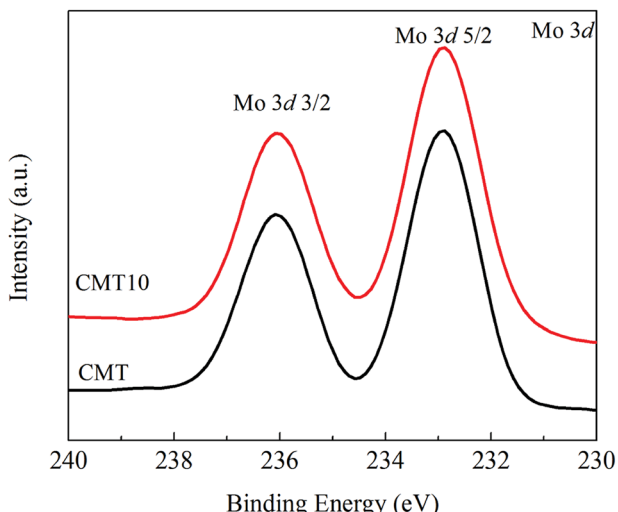
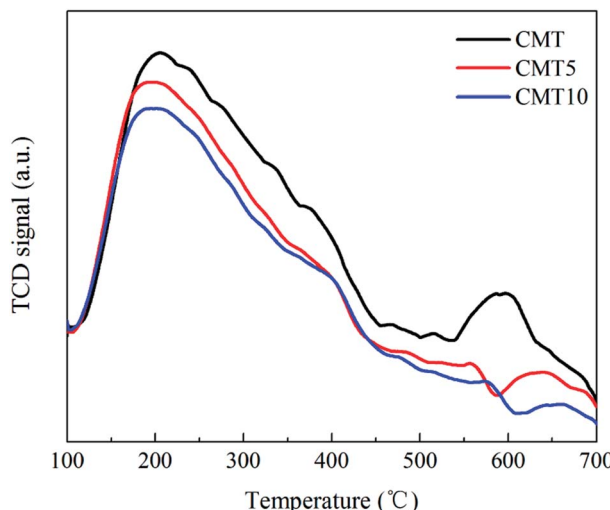
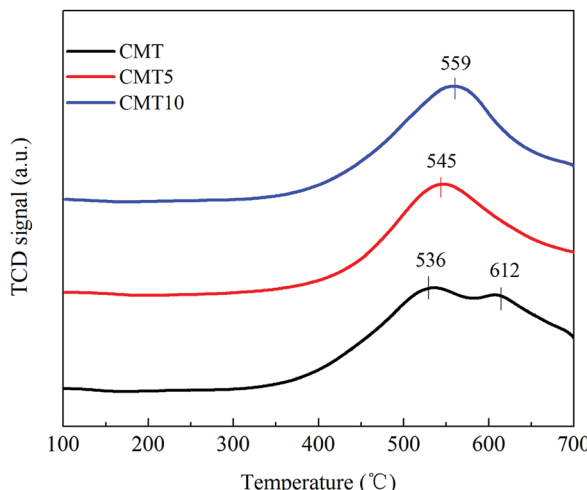


Fig. 10 XPS spectra of Mo 3d for the catalyst samples.

The presence of HCl could result in the transformation of Ce^{4+} into Ce^{3+} . However, Ce^{3+} in the form of CeCl_3 lost the ability to be converted into active Ce^{4+} and was unreactive in SCR reaction. Therefore, the $\text{Ce}^{3+}/\text{Ce}^{4+}$ redox cycle was damaged. It is generally accepted that the redox pairs of $\text{Ce}^{3+}/\text{Ce}^{4+}$ on catalyst surface are vital for the SCR reaction over CeO_2 -based catalyst.³³ As a result, the catalytic performance of CMT decreased.

The Mo XPS profiles of catalyst samples are shown in Fig. 10. The binding energies of $\text{Mo 3d}_{5/2}$ and $\text{Mo 3d}_{3/2}$ were observed at 232.6 and 235.9 eV, and both spectra of the catalysts provide typical patterns for MoO_3 .³⁴ Regardless of the peak positions or intensities, there was no obvious difference between CMT and CMT10 catalyst samples. It suggested that the chemical environment of Mo^{6+} remained almost the same after the introduction of Cl. Unlike active Ce species, MoO_3 supported on TiO_2 was not to be highly active for the SCR reaction.¹⁷ MoO_3 primarily acted as a structural and chemical promoter rather than main active species. Compared with the Ce and Mo XPS results, it could be supposed that HCl preferentially reacted with active Ce species instead of Mo species. Consequently, Mo XPS curve was not changed in the presence of HCl.

3.2.3 NH_3 -TPD analysis. NH_3 -TPD analysis was performed to study the surface acidity of the catalyst samples and the results are presented in Fig. 11. Each catalyst sample contained a broad NH_3 desorption peak centered at about 200 °C, which could be assigned to the weakly absorbed NH_3 on Brønsted acid sites.^{21,24} As for CMT, one small peak centered at about 600 °C was observed and could be attributed to the strongly absorbed NH_3 on Lewis acid sites.³⁵ The presence of HCl resulted in the decrease in the NH_3 desorption peak area at low and high temperatures. Furthermore, the peak at high temperature shifted to higher temperatures. It indicated that the Brønsted acid sites and Lewis acid sites on the surface of CMT decreased, thereby inhibiting the adsorption of NH_3 species on the catalyst. As a result, HCl has a negative effect on the activity of CMT.

Fig. 11 NH₃-TPD profiles of the catalyst samples.Fig. 12 H₂-TPR profiles of the catalyst samples.

3.2.4 H₂-TPR analysis. Apart from the surface acidity of the catalyst, redox property is also another key factor which influences the performance of SCR catalyst. Fig. 12 illustrated the H₂-TPR profiles of the catalyst samples. The TPR of the fresh CMT illustrated two overlapping reduction peaks, at 536 °C and 612 °C, indicating the co-reduction of surface Ce and well dispersed octahedral Mo species.^{36,37} After adding HCl, the peak at 612 °C disappeared while the peak at 536 °C moved to higher temperature. It was possible that the introduction of HCl make the two peaks overlap. Jin *et al.*³⁸ reported the similar phenomenon on CeO₂/TiO₂ catalyst with the modulation of HF. Nevertheless, the H₂ consumption decreased in the order: CMT > CMT5 > CMT10. It indicated that reducibility of CMT was weakened due to the presence of HCl. It was clear that HCl should be responsible for the strong inhibition in the catalytic activity of CMT.

4. Conclusions

In this work, the influence of HCl on the selective catalytic reduction of NO with NH₃ over CeO₂-MoO₃/TiO₂ catalyst was investigated. The experimental results showed that HCl had a negative effect on the SCR performance of CeO₂-MoO₃/TiO₂ catalyst. The presence of HCl led to pore blockage, weakened interaction among CeO₂, MoO₃ and TiO₂, reduction in surface acidity and degradation of redox ability. Though the amount of Ce³⁺ increased on the catalyst surface after adding HCl, Ce³⁺ in the form of CeCl₃ was not active in SCR reaction. The Ce³⁺/Ce⁴⁺ redox cycle was damaged. In addition, the concentration of surface Ce and Mo atoms and the amount of chemisorbed oxygen were found to decrease. All of these factors were responsible for the deactivation by HCl of CMT.

Conflicts of interest

There are no conflicts to declare.

Acknowledgements

This work was supported by the National Natural Science Foundation of China (No. 51506226), Natural Science Foundation of Shandong Province (No. ZR2015EM010), “the Fundamental Research Funds for the Central Universities” (No. 15CX05005A) and the scholarship from China Scholarship Council, China (CSC) (No. 201706455013).

References

- 1 H. Chang, X. Chen, J. Li, L. Ma, C. Wang, C. Liu, W. S. Johannes and J. Hao, Improvement of activity and SO₂ tolerance of Sn-modified MnO_x-CeO₂ catalysts for NH₃-SCR at low temperatures, *Environ. Sci. Technol.*, 2013, **47**(10), 5294–5301.
- 2 X. Du, J. Xue, X. Wang, Y. Chen, J. Ran and L. Zhang, Oxidation of sulfur dioxide over V₂O₅/TiO₂ catalyst with low vanadium loading: a theoretical study, *J. Phys. Chem. C*, 2018, **122**(8), 4517–4523.
- 3 L. Lietti, I. Nova and P. Forzatti, Selective catalytic reduction (SCR) of NO by NH₃ over TiO₂-supported V₂O₅-WO₃ and V₂O₅-MoO₃ catalysts, *Top. Catal.*, 2000, **11–12**, 111–122.
- 4 C. Tang, H. Zhang and L. Dong, Ceria-based catalysts for low-temperature selective catalytic reduction of NO with NH₃, *Catal. Sci. Technol.*, 2016, **6**(5), 1248–1264.
- 5 R. Guo, P. Sun, W. Pan, M. Li, S. Liu, X. Sun, S. Liu and J. Liu, A highly effective MnNdO_x catalyst for the selective catalytic reduction of NO_x with NH₃, *Ind. Eng. Chem. Res.*, 2017, **56**(44), 12566–12577.
- 6 X. Gao, X. Du, L. Cui, Y. Fu, Z. Luo and K. Cen, A Ce–Cu–Ti oxide catalyst for the selective catalytic reduction of NO with NH₃, *Catal. Commun.*, 2010, **12**(4), 255–258.
- 7 W. Shan, F. Liu, Y. Yu and H. He, The use of ceria for the selective catalytic reduction of NO_x with NH₃, *Chin. J. Catal.*, 2014, **35**, 1251–1259.



8 Z. Liu, H. Su, J. Li and Y. Li, Novel $\text{MoO}_3/\text{CeO}_2\text{-ZrO}_2$ catalyst for the selective catalytic reduction of NO_x by NH_3 , *Catal. Commun.*, 2015, **65**, 51–54.

9 Z. Liu, Y. Yi, J. Li, S. Woo, B. Wang, X. Cao and Z. Li, A superior catalyst with dual redox cycles for the selective reduction of NO_x by ammonia, *Chem. Commun.*, 2013, **49**(70), 7726–7728.

10 Z. Liu, J. Zhu, J. Li, L. Ma and S. Woo, Novel Mn-Ce-Ti mixed-oxide catalyst for the selective catalytic reduction of NO_x with NH_3 , *ACS Appl. Mater. Interfaces*, 2014, **6**, 14500–14508.

11 Y. Jiang, Z. Xing, X. Wang, S. Huang, Q. Liu and J. Yang, MoO_3 modified $\text{CeO}_2/\text{TiO}_2$ catalyst prepared by a single step sol-gel method for selective catalytic reduction of NO with NH_3 , *J. Ind. Eng. Chem.*, 2015, **29**, 43–47.

12 J. P. Chen, M. A. Buzanowski, R. T. Yang and J. E. Cichanowicz, Deactivation of the vanadia catalyst in the selective catalytic reduction process, *J. Air Waste Manage. Assoc.*, 1990, **40**(10), 1403–1409.

13 L. Lisi, G. Lasorella, S. Malloggi and G. Russo, Single and combined deactivating effect of alkali metals and HCl on commercial SCR catalysts, *Appl. Catal., B*, 2004, **50**(4), 251–258.

14 N. Z. Yang, R. T. Guo, W. G. Pan, *et al.* The deactivation mechanism of Cl on Ce/TiO_2 catalyst for selective catalytic reduction of NO with NH_3 , *Appl. Surf. Sci.*, 2016, **378**, 513–518.

15 Y. Hou, G. Cai, Z. Huang, X. Han and S. Guo, Effect of HCl on $\text{V}_2\text{O}_5/\text{AC}$ catalyst for NO reduction by NH_3 at low temperatures, *Chem. Eng. J.*, 2014, **247**, 59–65.

16 X. Yu, F. Cao, X. Zhu, X. Zhu, X. Gao, Z. Luo and K. Cen, Selective catalytic reduction of NO over Cu-Mn/OMC catalysts: effect of preparation method, *Aerosol Air Qual. Res.*, 2017, **17**, 302–313.

17 Y. Jiang, X. Zhang, M. Lu, C. Bao, G. Liang, C. Lai, W. Shi and S. Ma, Activity and characterization of Ce-Mo-Ti mixed oxide catalysts prepared by a homogeneous precipitation method for selective catalytic reduction of NO with NH_3 , *J. Taiwan Inst. Chem. Eng.*, 2018, **86**, 133–140.

18 M. Casapu, O. Kröcher and M. Elsener, Screening of doped $\text{MnO}_x\text{-CeO}_2$ catalysts for low-temperature NO-SCR, *Appl. Catal., B*, 2009, **88**, 413–419.

19 W. Xu, H. He and Y. Yu, Deactivation of a Ce/TiO_2 catalyst by SO_2 in the selective catalytic reduction of NO by NH_3 , *J. Phys. Chem.*, 2009, **113**, 4426–4432.

20 Y. Peng, C. Liu, X. Zhang and J. Li, The effect of SiO_2 on a novel $\text{CeO}_2\text{-WO}_3/\text{TiO}_2$ catalyst for the selective catalytic reduction of NO with NH_3 , *Appl. Catal., B*, 2013, **140–141**, 276–282.

21 P. Wang, Q. S. Wang, X. X. Ma, R. T. Guo and W. G. Pan, The influence of F and Cl on Mn/TiO_2 , catalyst for selective catalytic reduction of NO with NH_3 : a comparative study, *Catal. Commun.*, 2015, **71**, 84–87.

22 X. Wu, W. Yu, Z. Si and D. Weng, Chemical deactivation of $\text{V}_2\text{O}_5\text{-WO}_3/\text{TiO}_2$ SCR catalyst by combined effect of potassium and chloride, *Front. Environ. Sci. Eng.*, 2013, **7**(3), 420–427.

23 X. Gao, Y. Jiang, Y. Zhong, Z. Luo and K. Cen, The activity and characterization of $\text{CeO}_2\text{-TiO}_2$ catalysts prepared by the sol-gel method for selective catalytic reduction of NO with NH_3 , *J. Hazard. Mater.*, 2010, **174**(1–3), 734–739.

24 X. Du, X. Gao, L. Cui, Y. Fu, Z. Luo and K. Cen, Investigation of the effect of Cu addition on the SO_2 -resistance of a CeTi oxide catalyst for selective catalytic reduction of NO with NH_3 , *Fuel*, 2012, **92**(1), 49–55.

25 Y. Peng, K. Li and J. Li, Identification of the active sites on $\text{CeO}_2\text{-WO}_3$ catalysts for SCR of NO_x with NH_3 : an *in situ* IR and Raman spectroscopy study, *Appl. Catal., B*, 2013, **140–141**, 483–492.

26 N. Z. Yang, R. T. Guo, W. G. Pan, Q. L. Chen, Q. S. Wang and C. Z. Lu, The promotion effect of Sb on the Na resistance of Mn/TiO_2 catalyst for selective catalytic reduction of NO with NH_3 , *Fuel*, 2016, **169**, 87–92.

27 H. Chang, J. Li, J. Yuan, L. Chen, Y. Dai, A. Hamidreza, J. Xu and J. Hao, Ge, Mn-doped $\text{CeO}_2\text{-WO}_3$ catalysts for $\text{NH}_3\text{-SCR}$ of NO_x : effects of SO_2 and H_2 regeneration, *Catal. Today*, 2013, **201**(1), 139–144.

28 W. Shan, F. Liu, H. He, X. Shi and C. Zhang, A superior Ce-W-Ti mixed oxide catalyst for the selective catalytic reduction of NO_x with NH_3 , *Appl. Catal., B*, 2012, **115–116**, 100–106.

29 D. Devaiah, D. Jampaiah, P. Saikia and B. M. Reddy, Structure dependent catalytic activity of $\text{Ce}_{0.8}\text{Tb}_{0.2}\text{O}_{2-\delta}$ and TiO_2 supported $\text{Ce}_{0.8}\text{Tb}_{0.2}\text{O}_{2-\delta}$ solid solutions for CO oxidation, *J. Ind. Eng. Chem.*, 2014, **20**(2), 444–453.

30 R. T. Guo, C. Z. Lu, W. G. Pan, W. L. Zhen, Q. S. Wang, Q. L. Chen, H. L. Ding and N. Z. Yang, A comparative study of the poisoning effect of Zn and Pb on Ce/TiO_2 catalyst for low temperature selective catalytic reduction of NO with NH_3 , *Catal. Commun.*, 2015, **59**, 136–139.

31 F. Y. Chang, J. C. Chen and M. Y. Wey, Activity and characterization of $\text{Rh/Al}_2\text{O}_3$ and $\text{Rh-Na/Al}_2\text{O}_3$ catalysts for the SCR of NO with CO in the presence of SO_2 and HCl , *Fuel*, 2010, **89**(8), 1919–1927.

32 C. Wagner, W. Riggs, L. Davis, J. Moulder and G. Muilenberg, *Hand book of X-Ray Photoelectron Spectroscopy*, Perkin-Elmer Corporation, 1st. minnesota, 1979.

33 X. Li, X. Li, J. Li and L. Hao, Identification of the arsenic resistance on MoO_3 doped $\text{CeO}_2/\text{TiO}_2$ catalyst for selective catalytic reduction of NO_x with ammonia, *J. Hazard. Mater.*, 2016, **318**, 615–622.

34 H. L. Koh and H. K. Park, Characterization of $\text{MoO}_3\text{-V}_2\text{O}_5/\text{Al}_2\text{O}_3$ catalysts for selective catalytic reduction of NO by NH_3 , *J. Ind. Eng. Chem.*, 2013, **19**(1), 73–79.

35 R. Zhang, Q. Zhong, W. Zhao, *et al.* Promotional effect of fluorine on the selective catalytic reduction of NO with NH_3 over $\text{CeO}_2\text{-TiO}_2$ catalyst at low temperature, *Appl. Surf. Sci.*, 2014, **289**(289), 237–244.

36 Z. Liu, S. Zhang, J. Li and L. Ma, Promoting effect of MoO_3 on the NO_x reduction by NH_3 over $\text{CeO}_2/\text{TiO}_2$ catalyst studied with *in situ* DRIFTS, *Appl. Catal., B*, 2014, **144**(1), 90–95.



37 L. Caero, A. Romero and J. Ramirez, Niobium sulfide as a dopant for Mo/TiO₂ catalysts, *Catal. Today*, 2003, **78**, 513–518.

38 Q. Jin, Y. Shen and S. Zhu, Effect of fluorine additive on CeO₂(ZrO₂)/TiO₂ for selective catalytic reduction of NO by NH₃, *J. Colloid Interface Sci.*, 2017, **487**, 401–409.

